Bearing fault indicator in induction machine using stator current spectral analysis

Baptiste Trajin, Jérémi Regnier, Jean Faucher

Bearing Fault indicator in Induction Machine Using Stator Current Spectral Analysis

Baptiste Trajin*, Jérémi Regnier*, Jean Faucher*

*Université de Toulouse; LAPLACE; CNRS, INPT, UPS;
2 rue Charles Camichel BP 7122
31071 Toulouse cedex 07, France
Email: baptiste.trajin@laplace.univ-tlse.fr, jeremi.regnier@laplace.univ-tlse.fr, jean.faucher@laplace.univ-tlse.fr

Keywords: Bearing fault, Vibration spectrum analysis, Current spectrum analysis, Automatic energy extraction.

Abstract

This paper deals with the application of motor current spectral analysis for the detection of rolling bearings damage in asynchronous machines. Vibration measurement is widely used to detect faulty operations. However, this approach is expensive and cannot always be performed. An alternative is to base the monitoring on electrical quantities such as the machine stator current which is often already measured for control and detection purposes. Firstly, to define an automatic detector for bearing faults based on mechanical quantities, vibration spectra are analyzed. Afterwards, it is shown that bearing faults induce mechanical load torque oscillations. Then, a theoretical stator current model in case of load torque oscillations demonstrates the presence of phase modulation. Related sideband components on current spectrum can be used for detection. Experimental measurements show that a transfer function including resonance links amplitudes of sideband components to the torque oscillation frequency. This singularity will be used to improve the detection efficiency. A fault detector using the energy of stator current in specific frequency ranges is then proposed. The efficiency of the detector is studied for different operating conditions. The supply frequency values are particulary investigated to demonstrate that using the resonance previously described could improve detection performances.

1 Introduction

Electrical drives using induction motors are widely used in many industrial applications because of their low cost and high robustness. However, faulty operations could be induced by bearing faults [8, 10]. A condition monitoring allows improving the availability and reliability of the drive. Traditionally, bearing faults detection uses vibration analysis but measuring such mechanical quantities to detect bearing faults is often expensive. To reduce the cost of monitoring, available electrical quantities such as stator current could be used. A general review of monitoring and fault diagnosis schemes using stator current can be found in [6]. In case of bearing faults, several studies demonstrate that specific signatures appear on stator current spectrum [7, 11]. Therefore, few of them concern the definition of a detector performing an automatic extraction of relevant information from the current spectrum. The present work deals with these specific aspects.

In section 2, a short overview of bearing faults is presented. The principles of an automatic extraction of energy in vibration spectrum are defined and validated. In section 3, a particular approach based on the assumption that bearing faults induce load torque oscillations is studied [2]. Using the magnetomotive force theory, an analytical stator current model is used to demonstrate that sideband components due to load torque oscillations exist in the current spectrum. An experimental Bode diagram is determined to study the amplitude of these specific sidebands related to torque oscillation frequencies. In section 4, an automatic detector based on current spectral energy estimation in specific frequency ranges is presented. Finally, section 5 demonstrates the ability of the proposed detection scheme to distinguish healthy from faulty bearings for different operating conditions.

2 Vibration analysis for faulty bearings

2.1 Bearing faults and characteristic frequencies

6208-type bearings are modified using electro-erosion to create an outer or inner race 3mm-long single point defect comparable to the effect of spalling due to a severe ineffective lubrification [3]. Thus, faulty bearings are mounted in a $5.5kW$ induction machine supplied by a variable frequency inverter. An acquisition board is used to sample the torque, vibrations and stator currents. Characteristic frequencies of faulty bearings in the vibration spectrum are theoretically well known. Only the low frequency ranges ($< 1kHz$) are analyzed. In fact, low frequencies render defect which are related to the rotating speed like eccentricity or bearing faults. Moreover, low frequency harmonics due to defects could appear as combinations of mechanical rotating frequency. This characteristic frequencies can be expressed using (1) [4, 10].

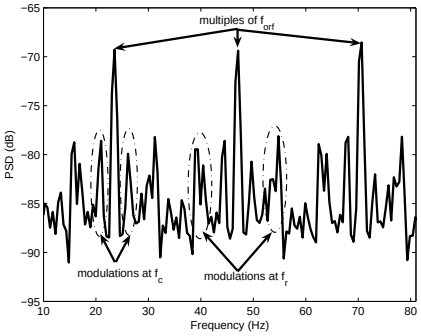

Figure 1: Vibration spectrum for outer race fault

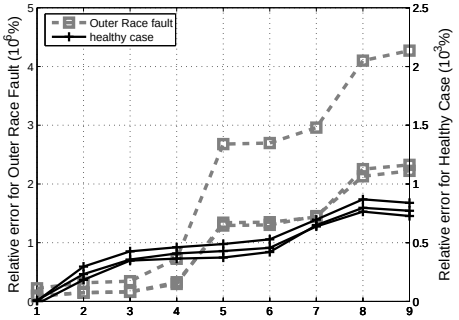

Figure 2: Mechanical indicator for outer race fault

$$
\begin{aligned}
f_{orf} &= \frac{f_r}{2} N_b \Big(1 - \frac{D_b \cos\theta}{D_p}\Big) \\
f_{irf} &= \frac{f_r}{2} N_b \Big(1 + \frac{D_b \cos\theta}{D_p}\Big) \\
f_c &= \frac{f_r}{2} \Big(1 - \frac{D_b \cos\theta}{D_p}\Big)
\end{aligned} \tag{1}
$$

where:

- f_{orf} outer race fault frequency;
- f_{irf} inner race fault frequency;
- f_c cage frequency;
- f_r mechanical rotating frequency;
- N_b number of balls;
- D_b ball diameter;
- D_p pitch diameter;
- θ contact angle.

2.2 Vibration spectrum and spectral energy detector

In case of outer race fault, vibration spectrum is computed using an averaged periodogram [5]. For example, Fig. 1 demonstrates that characteristic fault frequencies occur in vibration spectrum. Here, the supply frequency is chosen equaled to $13.3Hz$. Considering the slip of the induction machine, the mechanical rotating frequency is then equal to $6.56Hz$. Using (1) and the assumption that the contact angle is null (no axial load applied on the rotor shaft), the cage frequency equals $f_c = 2.61Hz$ and the outer race fault frequency equals $f_{orf} = 23.5Hz$. Obviously, combinations of several fault frequencies appear in the vibration spectrum. Strong modulations at f_c and f_r can be noticed around the multiples of outer race fault frequency.

These observations lead us to define a mechanical detector based on spectral energy in vibration spectrum. The fault detector is defined by extracting energies on frequency ranges related to the frequency components at f_{def}, where f_{def} is either the inner or the outer race theoretical fault frequency. Moreover, the frequency ranges are extended to include modulations linked to the mechanical speed and cage frequencies underlined by the vibration spectral analysis (see Fig. 1). The chosen frequency ranges are given in (2). The proposed indicator uses the relative energy error in the specified frequency ranges between a faulty and healthy reference vibration spectrum. A cumulative sum is then applied on the energy differences extracted from the frequency ranges related to the bearing fault investigated.

$$
\begin{gathered}
[nf_{def} - f_c; nf_{def} + f_c] \\
[nf_{def} - f_r - f_c; nf_{def} - f_r + f_c] \\
[nf_{def} + f_r - f_c; nf_{def} + f_r + f_c]
\end{gathered} \tag{2}
$$

where $n \in [1; 3]$.

Fig. 2 presents this indicator for $f_{def} = f_{orf}$. Notice that Fig. 2 is double scaled with a factor of 1000 between the two vertical axes. Using a common healthy reference, the cumulative sum of the energy difference for an outer race fault and a healthy case are compared. The distinction between healthy and faulty case can thus be clearly done. This approach certifies that bearing fault detection is possible using the energy in the spectrum of mechanical quantities. However, setting $f_{def} = f_{orf}$ or $f_{def} = f_{irf}$ does not guarantee the distinction between inner and outer race faults. In fact, numerous harmonics due to inner race defect exists in frequency ranges corresponding to outer race fault and reciprocally. Consequently, such an energy detector cannot be used for diagnosis but only for detection and monitoring of bearing faults. This observation is not really a negative point because many applications do not require an accurate diagnosis of the bearing defect.

3 Load torque oscillations

3.1 Load torque oscillations due to bearing faults

After demonstrating the effects of bearing faults on vibrations in section 2, the effects of bearing faults on mechanical load torque are required. Experimental spectrum of load torque demonstrates the presence of harmonics at frequencies related to bearing faults. Here, the mechanical speed is chosen equal to the nominal one namely $25Hz$. The outer race fault frequency equals $89Hz$ and the inner race frequency equals $136Hz$.

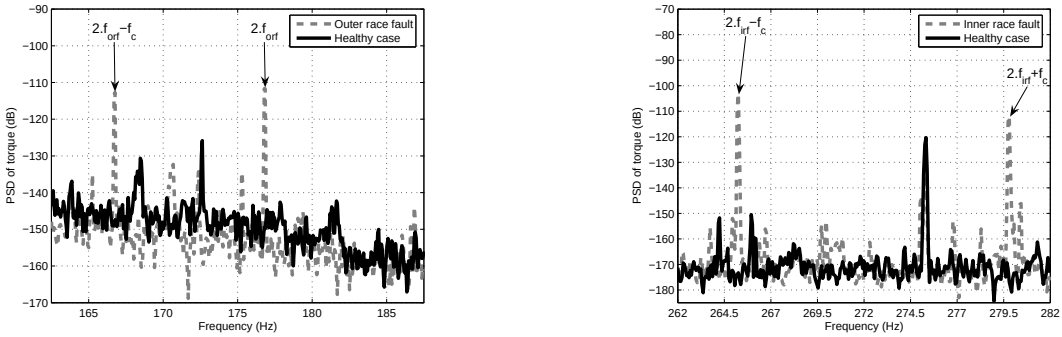

(a) (b)

Figure 3: Spectrum of mechanical torque - Comparison between healthy and faulty cases

Hence, Fig. 3(a) and 3(b) show a part of the mechanical torque spectrum around twice the characteristic fault frequency for outer and inner race fault respectively compared to the healthy case. It could be noticed that bearing defects cause some load torque oscillations which can be detect by a mechanical measure. In the following part, the link between load torque oscillations and stator current will be recalled.

3.2 Stator current model

Previous studies on mechanical failures in induction motors have shown that load torque oscillations induce phase modulations (PM) on stator current [1, 2, 9]. Considering that the load torque oscillation is composed of a single harmonic at the pulsation ω_{osc}, the load torque on the shaft of the machine can be expressed using (3) as an average torque equal to the electromagnetic motor torque and a sinusoidal component of amplitude Γ_c :

$$\Gamma_{load}(t) = \Gamma_0 + \Gamma_c \cos(\omega_{osc} t) \tag{3}$$

Physically, considering the mechanical equation linking torque to mechanical angular position, it is proved that load torque oscillations cause angular position oscillations. Here, the mechanical transfer function is equal to a simple inertia plus an integrator. The mechanical position is used to calculate the rotor magnetomotive forces (MMF). Thus, magnetic field in airgap is obtained by the product between the airgap permeance Λ_0, considered as a constant (along time and position), and the rotor and stator MMF. The magnetic field is integrated on the coil's surface of a stator winding in order to determine the airgap flux density in the coil. Hence, time derivation of airgap flux density in a stator winding leads to induced voltage. The stator current expression (4) for an arbitrary phase is then obtained considering a linear relation between current and induced voltage. In (4), I_s is the amplitude of stator current, I_r the amplitude of rotor current, p the number of pole pairs of the asynchronous machine and J the inertia.

$$i(t) = I_s \cos(\omega_s t + \phi_s) + I_r \sin\left(\omega_s t + p\frac{\Gamma_c}{J\omega_{osc}^2}\cos(\omega_{osc} t)\right) \tag{4}$$

In (4), the first term is related to the stator MMF contribution and the second one, including the phase modulation of stator current, is related to the rotor MMF contribution. If the amplitude of the torque oscillation is pretty slight, the Fourier Transform (FT) of the stator current can be expressed using (5) along the frequency ν.

$$FT\{i(t)\} = (I_s + I_r)\delta(\nu - f_s) + I_r p\frac{\Gamma_c}{2J\omega_{osc}^2}\delta\Big(\nu - (f_s \pm f_{osc})\Big) \tag{5}$$

Moreover, notice that in case of faulty bearings, the frequency of load torque oscillations f_{osc} can equal any of combinations of characteristic fault frequencies underlined by the load torque spectrum.

3.3 Amplitude variation law of sideband components

The knowledge of the amplitude variation of stator current sideband components related to the fault frequency is of strong interest for detection purpose. The link between PM harmonics amplitudes of the stator current and load torque oscillation frequencies is then experimentally studied and compared to the theoretical expression (5).

In order to draw a Bode diagram, the asynchronous motor is coupled to a DC motor. The DC machine is connected to a resistor through a DC/DC converter which controls the DC motor armature current. The reference current is composed of an oscillating component plus an offset in order to induce load torque oscillation around a mean torque value. Mechanical torque is measured with a torque sensor. Sideband component amplitudes of stator current are measured by off-line spectral analysis. The experimental gain Bode diagram shown in Fig. 4 is obtained by varying frequency of load torque oscillations. The main observation lies in the existence of a resonance point around $f_{res} = 20Hz$. Assuming that a single-point

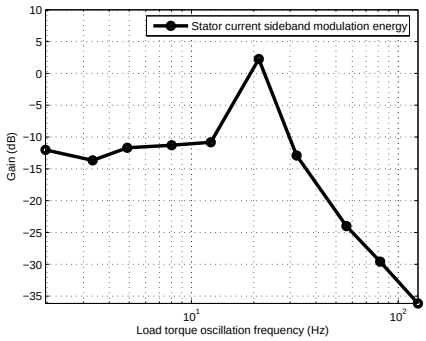

Figure 4: Gain Bode diagram of experimental transfer function between load torque oscillations frequency and sideband components on stator currents

defect related to characteristic frequencies determined in (1) creates slight load torque oscillations at these frequencies, the resonance point is used as a natural amplifier to obtain higher PM harmonics on stator current. Then, in order to use the resonance point, the supply frequency of the asynchronous machine is tuned to ensure that the theoretical mechanical fault frequency of the bearing under test equals the mechanical resonance noticed on the Bode diagram. In fact, with this approach, the PM modulation index shown in (5) will increase because of the resonance.

4 Definition of a current spectral detector for bearing faults

4.1 Improvement of SNR of stator current for fault harmonic detection

As defined in section 3, single-point defects induce load torque oscillations and consequently, phase modulations on stator current. However, amplitude of this PM is quite slight and could be buried in noise. Reducing the Signal to Noise Ratio (SNR) of the current signal is then necessary. On current measurements, noises are considered to be not correlated neither along time nor on two stator phases. Dividing the currents measurements into time blocks, the averaged periodogram allows reducing the SNR by correlating measurements. It can be estimated that the variance of the full signal is divided by the number of block used [5]. Moreover, the SNR can be improved and the noise variance reduced by correlating two phase currents using a multiplication of their Fourier Transform. As a consequence, the evaluated SNR of the resulting signal is twice the SNR of a unique current. This method allows improving the efficiency of fault harmonic detection. In common applications, measuring two stator currents is often performed for control purposes so this SNR reducing method does not require more sensor.

4.2 Definition of current spectral detector

The fault detector is defined by extracting energies on frequency ranges corresponding to the sideband components at $f_s \pm f_{def}$ where f_{def} is either the inner or the outer race theoretical fault frequency. Moreover, the frequency ranges are extended to include modulations linked to the mechanical speed and cage frequencies underlined by the vibration and mechanical load torque spectral analysis (see Fig. 1 and 3). The chosen frequency ranges are given in (6). The proposed indicator uses the relative error of energy between the current spectrum in faulty and healthy case in the specified frequency ranges.

$$\begin{array}{c} |f_s \pm [nf_{def} - f_c; nf_{def} + f_c]| \\ |f_s \pm [nf_{def} - f_r - f_c; nf_{def} - f_r + f_c]| \\ |f_s \pm [nf_{def} + f_r - f_c; nf_{def} + f_r + f_c]| \end{array} \quad (6)$$

where $n \in [1; 5]$, f_r is the mechanical rotating speed and f_c the characteristic cage frequency.

Then, as expressed in (7), the relative errors of energy extracted from outer and inner race fault frequencies ranges (ΔE_{orf} and ΔE_{irf} respectively) are added in order to get a single energy difference ΔE_{tot}.

$$\Delta E_{tot}(k) = \Delta E_{orf}(k) + \Delta E_{irf}(k) \quad (7)$$

Finally, a cumulative sum of $\Delta E_{tot}(k)$ is used to build the indicator. Only the last value of the cumulative sum is considered as the detector value. As a consequence, the final detector value could not perform a distinction between inner and outer race fault but only provide a distinction between healthy and faulty case. The detection of inner or outer race fault will only be done with the supply frequency which is tuned to equal the resonance frequency f_{res} and one of the characteristic fault frequencies (f_{orf} or f_{irf}).

5 Experimental Results

The acquisitions of the stator currents are done during $80s$ using a sampling frequency of $6400Hz$. As the analysis are performed off-line, the data size and computation time are not considered as constraints. Three experimental conditions are tested, corresponding to three different supply frequencies. Each case uses a reference of energy obtained with a healthy bearing.

5.1 Detection of outer race fault

In order to use the resonance point, the supply frequency f_s is tuned to $13.3Hz$ to ensure $f_{orf} = f_{res}$. The detection of outer race fault is then favored by the amplification due to the resonance. From Fig. 5(a), the representation of the cumulative sum allows differentiating outer race faulty conditions from the other cases. As expected, properly tuning the frequency supply leads to focus on outer race fault. When f_s is set to guarantee $f_{orf} = f_{res}$, the detection of the outer race fault is ensured.

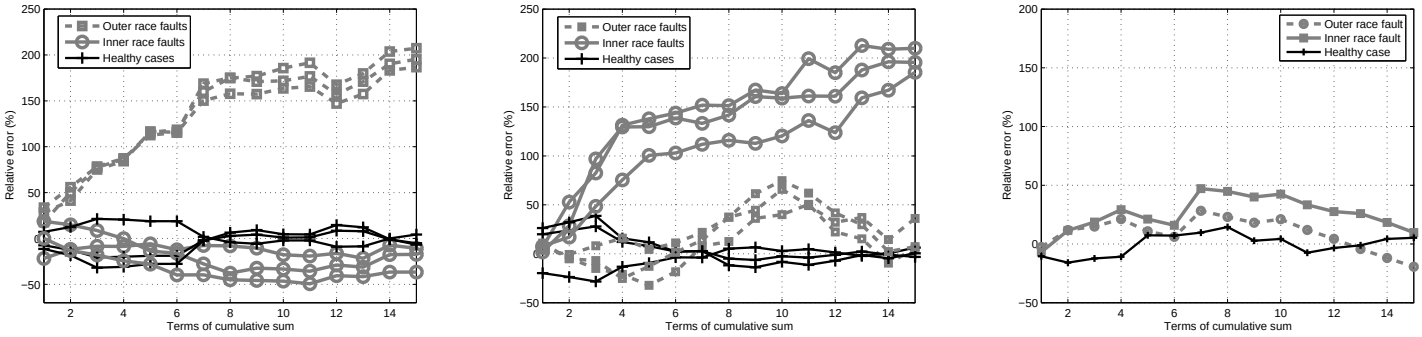

(a) $f_{orf} = f_{res}$ (b) $f_{irf} = f_{res}$ (c) $f_s = 50Hz$

Figure 5: Cumulative sums of relative error in %

5.2 Detection of inner race fault

In order to favor the detection of inner race fault, the supply frequency f_s is tuned to $6.7Hz$ to ensure $f_{irf} = f_{res}$. From Fig. 5(b), the representation of the cumulative sum allows differentiating inner race faulty conditions from the other cases. Once again, properly tuning the frequency supply leads to focus on the selected fault. Moreover, Fig. 5(a) - 5(b) underline that if the characteristic fault frequency does not equal the resonance frequency, the associated fault is not detected.

5.3 Detection of faults at nominal frequency

The supply frequency f_s is tuned to $50Hz$, corresponding to the nominal supply frequency of the machine. No characteristic fault frequencies are equaled to the resonance point. In this case, $f_{irf} = 136Hz$ and $f_{orf} = 89.4Hz$. The PM signatures are located in the attenuation part of the electromechanical transfer function (see Fig.4). Fig. 5(c) underlines that distinction between healthy and faulty cases is not possible with this detector when the sideband components are strongly attenuated. It emphasized the importance of properly tune the supply frequency to ensure the detection of a possible bearing fault.

6 Conclusion

In this paper, a novel method for an automatic detection of bearing fault in induction motors using stator current monitoring has been presented. As inner and outer race characteristic fault frequencies are well known, bearings are artificially damaged to ensure the assumption of single-point defect. A vibration spectrum analysis has been proposed to validate the principles of an automatic spectral detector based on the extraction of energy in frequency ranges related to bearing faults. Mechanical measurements have shown that bearing defects induced load torque oscillations. Thus, a model of stator current demonstrates that load torque oscillations lead to sideband components on stator current spectrum. The amplitude variation law of these signatures with respect to fault frequency has been determined by experimental measurements in order to refine the proposed stator current model. The exploitation of the resonance point allows detecting preferentially inner or outer race fault. A detector based on extraction of energy in frequency ranges related to PM signature in the stator current spectrum has been built. The automatic detector allows clearly distinguishing healthy and faulty cases with a good confidence rate while the supply frequency is tuned to ensure the detection by using the resonance point. To reduce the computation complexity and demonstrate the efficiency and reproducibility of the detector, short data length records will be studied in further work. Moreover, more realistic faults will also be investigated.

References

[1] M. Blodt, J. Faucher, B. Dagues and M. Chabert. "Mechanical load fault detection in induction motors by stator current time-frequency analysis", *IEEE International Conference on Electric Machines and Drives*, pp. 1881-1888, (May 2005).

[2] M. Blodt, P. Granjon, B. Raison and G. Rostaing. "Models for bearing damage detection in induction motors using stator current monitoring", *IEEE International Symposium on Industrial Electronics*, **volume 1**, pp. 383-388, (May 2004).

[3] R. A. Guyer. "Rolling Bearings Handbook and Troubleshooting Guide", *Chilton Book Compagny*, Radnor, Pennsylvania, (1996).

[4] T. A. Harris. "Rolling bearing analysis", *Wiley*, New-York, 3rd ed., (1991).

[5] S. M. Kay. "Modern Spectral Estimation: Theory and Application", *Prentice Hall*, Englewood Cliffs, New Jersey, (1988).

[6] S. Nandi and H. A. Toliyat. "Condition monitoring and fault diagnosis of electrical machines - a review", *IEEE Transactions on Energy Conversion*, **volume 20, no. 4**, pp. 719-729, (Dec. 2005).

[7] R. R. Obaid, T. G. Habetler and J. R. Stack. "Stator current analysis for bearing damage detection in induction motors", *Symposium on Diagnostics for Electric Machines, Power Electronics and Drives*, pp. 182-187, (Aug. 2003).

[8] B. Raison, G. Rostaing, O. Butscher and C. -S. Maroni. "Investigations of algorithms for bearing fault detection in induction drives", *IEEE 28th Annual Conference of the Industrial Electronics Society*, **volume 2**, pp.1696-1701, (Nov. 2002).

[9] R. R. Schoen and T. G. Habetler. "Effects of time-varying loads on rotor fault detection in induction machines", *IEEE Transactions on Industry Applications*, **volume 31, no. 4**, pp. 900-906, (Jul-Aug. 1995).

[10] J. R. Stack, T. G. Habetler and R. G. Harley. "Fault classification and fault signature production for rolling element bearings in electric machines", *IEEE Transactions on Industry Applications*, **volume 40, no. 3**, pp. 735-739, (May-Jun. 2004).

[11] J. R. Stack, R. G. Harley and T. G. Habetler. "An amplitude modulation detector for fault diagnosis in rolling element bearings", *IEEE Transactions on Industry Electronics*, **volume 51, no. 5**, pp. 1097-1102, (Oct. 2004).